Review

Relevant length scales in Brillouin imaging of biomaterials: the interplay between phonons propagation and light focalization

Maurizio Mattarelli, Massimo Vassalli, and Silvia Caponi

ACS Photonics, **Just Accepted Manuscript** • DOI: 10.1021/acsphotonics.0c00801 • Publication Date (Web): 31 Jul 2020

Relevant length scales in Brillouin imaging of biomaterials: the interplay between phonons propagation and light focalization

Maurizio Mattarelli[1], Massimo Vassalli [2], Silvia Caponi [31]*

[1] Dipartimento di Fisica e Geologia, Università di Perugia, Via A. Pascoli, I-06100 Perugia, Italy

[2] James Watt School of Engineering, University of Glasgow, Glasgow, UK

[3] Istituto Officina dei Materiali, National Research Council (IOM-CNR), Unit of Perugia, c/o Department of Physics and Geology, University of Perugia, Via A. Pascoli, I-06123 Perugia, Italy

Abstract

Recent advances in photonics technologies pushed optical microscopy towards new horizons in materials characterization. In this framework, Brillouin microscopy emerged as an innovative method to provide images of materials with mechanical contrast without any physical contact, but exploiting the light-matter interaction. Brillouin imaging holds a great promise; to allow mechanical analysis inside soft and heterogeneous materials, addressing the pivotal role played by viscoelastic properties in the physiology and pathology of living tissues and cells. Nevertheless, extending the approach of Brillouin imaging to characterize elastic heterogeneities of micro and nanostructured samples is especially challenging, and it poses a critical question about the actual spatial resolution reachable in the mechanical characterization. We focus this critical review on the key quantities that define the spatial resolution in the Brillouin scattering process, and we highlight that not only the optical focalization of the light, but also the acoustic excitations present in the material, influence the information collected from a sample by Brillouin imaging. Referring to the body of knowledge gained in the field of material science, we review new results and recently obtained progresses in the more unexplored context of life science. In future developments, a comprehensive strategy to tackle both the acoustic and optical aspects of the measurement will be required to maximize the efficacy of the technique.

Keywords: Biophotonics, Brillouin spectroscopy, spatial resolution, phonons, biomechanics, cell mechanics.

* corresponding author: silvia.caponi@cnr.it

Introduction

In recent years, a plethora of advanced photonic approaches has emerged, further extending traditional optical microscopy and providing a new representation of biological matter. Among others, Brillouin spectroscopy is particularly spreading, finding promising applications in biological and biomedical research. Brillouin spectroscopy is an almost century old technique[1,2] and it provides the unique ability to probe the mechanical properties of unstained samples without any physical contact. In fact, the elastic moduli of the material are gathered analyzing the scattering process between the photons of the light and the acoustic phonons present in the material. The application of Brillouin spectroscopy to biological systems provides a striking opportunity to shine light inside living tissue and decipher the complex mechanical interplay between the polymeric matrix and the embedded cells. The crucial role of tissue and organ biomechanics for human physiology and pathology is apparent in many contexts, from structural aspects in the musculoskeletal tissue, to dynamical considerations in the cardiovascular system. The pivotal role of viscoelastic properties in driving biological functionality has been recently recognized to a smaller scale, at the level of single cells and molecular complexes. The interest for the role of mechanics in cell biology, mechanobiology, has challenged traditional instrumentation for mechanical characterization at the micro-scale. The technological research has headed towards the development of new investigation methods able to reach the required spatial resolution. In this framework, micro-Brillouin spectroscopy has been proposed as a promising biophotonic tool. Cell biology[3–6], plant biology[7], ophthalmology[8,9], cancer cell mechanics[10,11] or tissue biomechanics [12–17] are only some examples of biomedical fields recently approached by this technique.

The inherent heterogeneity of biological samples affects all length scales, from the tissue level, down to the size of cells and subcellular structures. When the structural length scale of the sample matches the characteristic size of the phonons, the peculiar interplay between the light and the acoustic field - at the basis of Brillouin Scattering - has to be carefully taken into account. This mechanism, together with the propagating nature of the phonons, is crucial for the correct interpretation of Brillouin spectra.

In order to address this issue, we propose to observe the phenomenon with a reductionist perspective, comparing the Brillouin characterization of biological materials with artificial inorganic ones. Synthetic materials can be designed to feature specific micro-structures, with defined geometry and mechanical properties, allowing to clearly decorrelate the characteristic features of the sample from the ones of the phononic and photonic fields.

Brillouin spectroscopy and mechanical imaging

When light goes across a transparent material, due to local and static fluctuations of the refractive index, it is elastically scattered in different directions in space. Additionally, if the refractive index fluctuations are also time dependent, related for example to the presence of molecular or collective vibrations, the scattered light will also undergo a frequency shift. Techniques based on inelastic light scattering processes, such as Raman and Brillouin spectroscopy, analyze the frequency shift of a monochromatic beam after the interaction with normal vibrational modes, disclosing the chemical and mechanical properties of the material.

While Raman spectroscopy is already considered an effective analytical tool in biological context[18], Brillouin spectroscopy extensively approached this field only in the last years [3–12] [13–17] [19–23] . The interest for Brillouin Light Scattering (BLS) originates from the possibility to evaluate the stiffness tensor and the viscoelastic properties of the sample from the measurements of the speed of propagation of the acoustic waves. In fact, both the longitudinal waves (due to density fluctuations) and the transverse waves (due to induced effects on the

polarizability) produce refractive index fluctuations measurable by BLS. Exploiting its contactless and label free character, BLS has been applied to different classes of systems, from inorganic crystals to amorphous materials, analyzing the influence on the elastic behavior of specific parameters, such as temperature, internal stresses, pressure and polymerization processes (see [24–27] and references therein). In pioneering works, BLS has been applied to study materials of biological relevance[28], analyzing their elastic anisotropy[29]. However, the accurate characterization of spatially heterogeneous materials, such as biological and biomedical samples, forced to extend the approach from single point investigation, significant only in homogeneous systems, toward the raster scan probing of the mechanics at the microscale. The first attempt to produce a Brillouin image has been realized more than 15 years ago[30], and this approach is reinforced in newly developed devices in terms of speed, spectral resolution and contrast. The use of single[6,15,31–33] or multiple Virtually Imaged Phase Array (VIPA)[3,13,34,35] or the use of stimulated Brillouin approach[36–39] strongly increased the acquisition speed. On the other hand, the use of avalanche photodiodes in the high contrast tandem Fabry-Perot interferometers increased the performance of more traditional systems[10,40]. The different experimental setups, till now proposed, show different abilities which run from the accurate linewidth analysis[10,12,40] to a remarkable acquisition speed[36,39,41] which allowed the in vivo analysis, supporting the development of Brillouin spectroscopy in biomedical fields[9].

As any other imaging technique, the main challenge of Brillouin imaging is its spatial resolution. In the case of micro-Brillouin spectroscopy, the spectrometer is coupled to an optical microscope used to focalize and collect the light from a sub micrometric scattering volume. However, for any investigation, the resolution depends both on the ability to control the probe and on the interaction processes between the probe and the sample. This can give rise to a complex scenario. A clear demonstration of that can be given when considering optical microscopy. In far-field light microscopy, the extent of the focal spot depends on the wavelength of the used light λ, and due to the Abbe's diffraction limit, it cannot be reduced under $\lambda/3$ in the lateral and λ in the axial direction. However, super-resolution imaging overcomes this constraint and structural details of nano-metric size can be directly detected. This is achieved by exactly tuning the interaction between the materials under investigation and the probe[42–45]. Some of these advantages can be exploited also in spectroscopic approaches. For example, in Raman micro-spectroscopy, the use of pointed probes[46] or nanoparticles confers enhanced plasmonic properties, allowing the chemical characterization of nano-metric structures or single molecules in low concentrated solutions.

In the case of BLS the scenario is much more complex. In fact, while Raman spectroscopy probes the single molecules vibrational modes, i.e. localized modes, Brillouin spectroscopy probes collective vibrations i.e. acoustic propagating long wavelength phonons. In this case, more than one length-scale has to be accounted for, to define the effective spatial resolution of the technique[47].

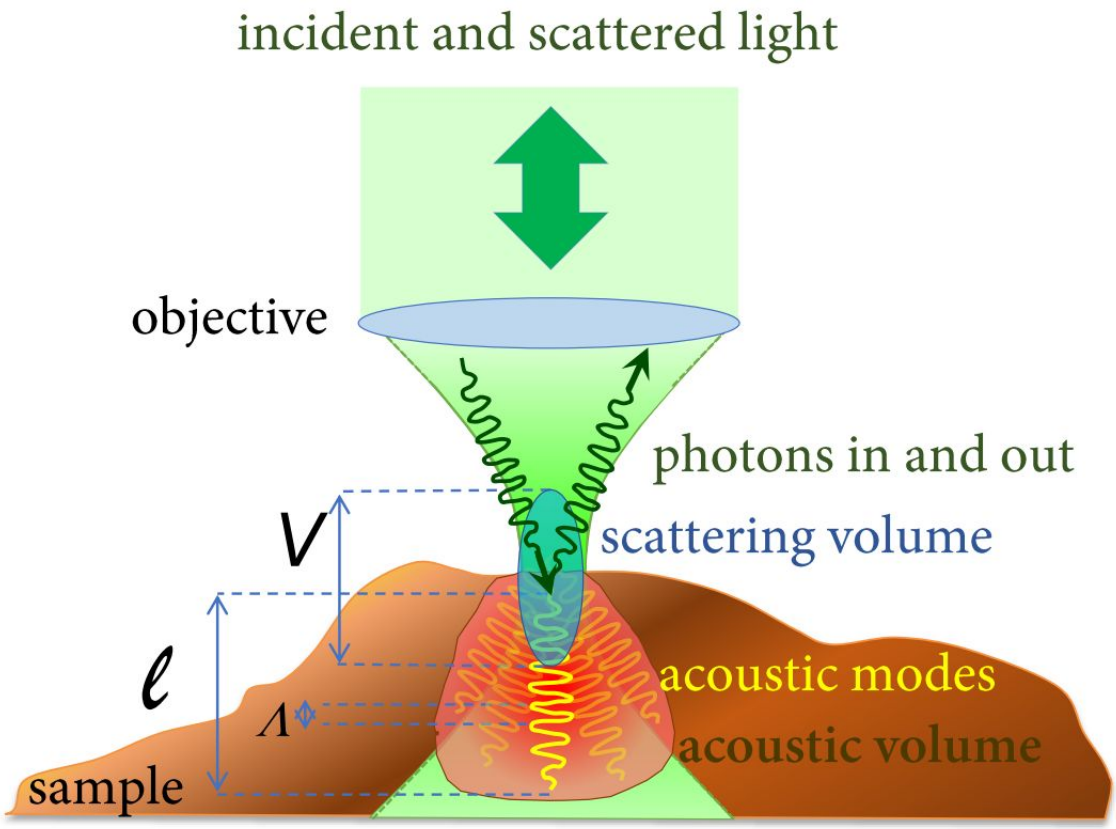

Figure 1: Micro-Brillouin scattering layout. Λ, ℓ, and V are the phonon wavelength, mean free path, and the characteristic size of the scattering volume, respectively. All these quantities have to be considered in the Brillouin scattering process. In red, the figure shows the acoustic volume, which takes into account the broadening related to the phonons propagation. Figure adapted with permission from ref. [47] © The Optical Society.

As with optical microscopy, one of the constraints to the resolution is the size of the focal spot, called in spectroscopy, scattering volume (indicated as V in Figure 1), which, for a given radiation wavelength, λ, depends on the focalization optics and on the transparency of the sample. In fact, in the case of opaque or non-transparent materials, the scattering volume will be reduced respect to the expected one by a factor depending on the optical penetration depth. Beside V, the wavelength of the investigated phonons (Λ), and their finite propagation length, ℓ, play a role and should be accurately considered (see Figure 1 for a representation of these length scales). With some discrepancies, the relevance of these different scales was highlighted and discussed in recent works[10,19,20,47,48], for the purpose of defining both the expected frequency spectrum and the accuracy by which the mechanical parameters of the sample are measured. This question is of the utmost importance, because in absence of such clarification, the data interpretation can be misleading.

Phonons propagation and attenuation

For the sake of simplicity, let's consider a lossless, elastically homogeneous, infinite medium. The acoustic normal mode, usually called phonon, in the most common representation takes the form of a plane wave with a definite wavelength and frequency. In this case, the propagating length scale extends on the infinite distance. Real media, however, are neither homogeneous at all length scales nor without internal dissipation processes. Under these conditions, any elastic excitation is characterized by a finite propagation length. This excitation, limited in space and time, is still called a phonon, even if improperly, and the phonon lifetime and propagation length are the time and space intervals in which it exists. The finiteness of the phonon brings a consequence - ultimately related to the Uncertainty Principle - that phonons are no longer monochromatic waves, but wave packets with a spread in frequency.

In any Brillouin experiment, the scattering geometry selects a well-defined exchanged wave-vector, q, probing only the phonons traveling in a given direction with a given wavelength, $\Lambda = 2\pi/q$. In micro-spectroscopy setups, the back-scattering configuration is usually used. In this case, the previous relation is simplified to $\Lambda=\lambda/2n$, n being the material refractive index. In this case, the detected phonons mainly propagate along the axial direction, which is also the direction where the elastic properties are measured. Under this assumption, the spectrum of the scattered light shows the elastic line flanked by equally shifted Stokes and anti-Stokes Brillouin peaks. In materials where the attenuation processes are not negligible, the Brillouin peaks are modeled by a damped harmonic oscillator, DHO[49]:

$$I(\omega) = \frac{I_0}{\pi} \frac{\omega_B^2 \Gamma}{\left(\omega^2 - \omega_B^2\right)^2 + \omega^2 \Gamma^2} \quad (1)$$

where the frequency position of the Brillouin peaks, ω_B, is associated with the elastic component, while Γ, the ω-spread of the phonons, is the viscous term. In particular, ω_B is linearly linked to the longitudinal sound velocity, v, $\omega_B = vq$, and in turn, related to the longitudinal elastic modulus $M' = \rho\, \omega_B{}^2/q^2$. Similarly, Γ relates to the average propagation length (or mean free path) $\ell = v/\Gamma = \omega_B/\Gamma\ \Lambda$[27]. In low attenuation regimes, the DHO is well approximated by two symmetrically shifted Lorentzian curves[49] , which are often used to model the experimental spectra. In the analysis of complex viscoelastic materials, both the frequency and the width of the Brillouin peak are important quantities, not only to characterize the sample properties, but also to evaluate the spatial resolution of the mechanical characterization. Note that the collected spectrum is the result of the sample signal convoluted with the instrumental response function, which is influenced both by the frequency resolution and by the accuracy in the q-selection[9]. Both effects have to be considered before actually evaluating the attenuation, Γ.

In general, the width of the Brillouin peak takes into account all the different phonon attenuation processes active in the materials. Depending on their microscopic origin, they are usually classified as dynamic or static processes[50]. In the case of dynamic mechanisms, the phonon energy is exchanged with the internal degrees of freedom of the materials. This process is particularly relevant in homogeneous viscoelastic samples, where the origin of this broadening is associated with intrinsic material properties, i.e. the viscous response of the sample. In absence of other phonon attenuation processes, it turns out that $\Gamma = \eta_L q^2$ [26,48,50], where η_L is the kinematic viscosity. Furthermore, in the case of the static process, the phonons pathway is hindered by the presence of elastic heterogeneities in the materials. This mechanism strongly depends on the length scale of the heterogeneities, and it is the main focus of this review.

From the elastic continuum to elastically heterogeneous systems at micro and nanoscales

In the following, we will consider the features of the Brillouin spectrum acquired in a few selected classes of inorganic materials, mainly based on vitreous silica, v-SiO_2, for which a huge amount of data is available, due to its technological relevance. As such materials can be rather easily fabricated with varying spatial distribution of the constituents, it is possible to highlight the effect of the mechanical discontinuities in the Brillouin spectra. In fact, the introduction of elastic defects in a continuum medium[51,52] affects the phonons propagation: the relative ratio between the heterogeneity size and the phonon wavelength is the key parameter to explain the modifications in the phonon mean free path, ℓ. To address the impact of the length scale, different material geometries have been considered, from a homogeneous glass to a matrix with pores of controlled size, ultimately reaching an aggregation of particles. These systems are depicted in the left side of Figure 2, while the right side refers to the equivalent-scale biological counterpart, presented in the next paragraph.

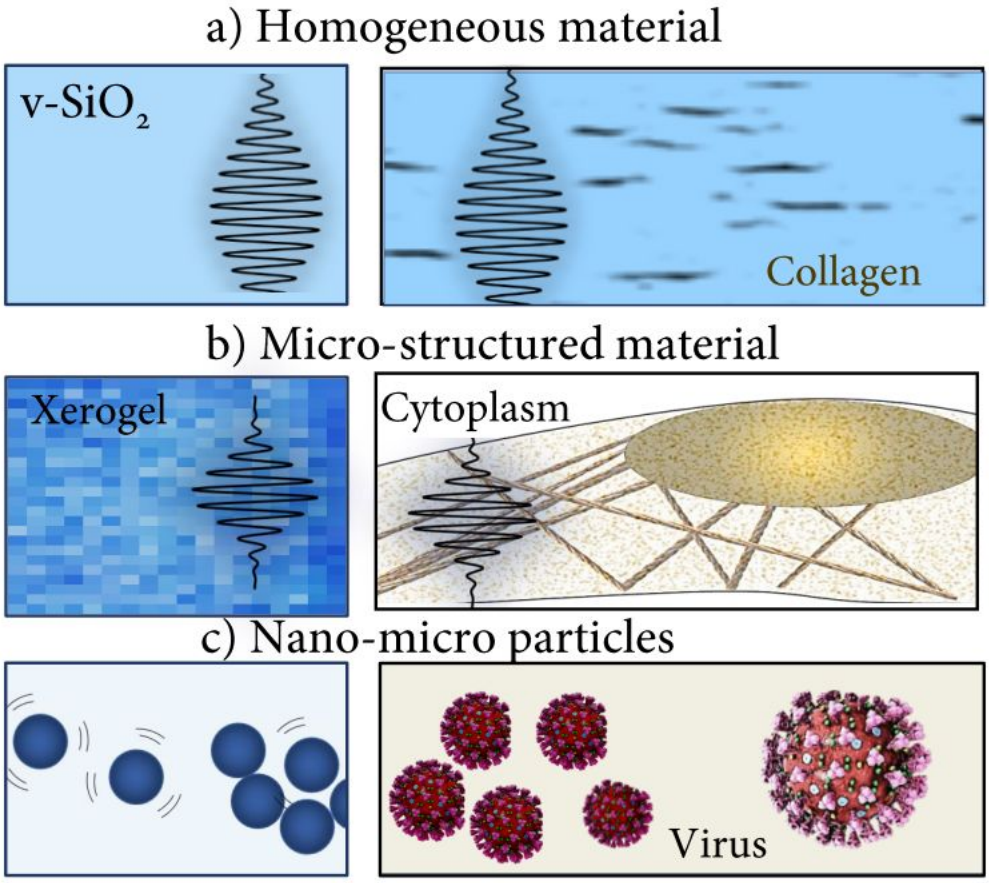

Figure 2: The length scale of heterogeneities in the sample morphology has to be compared with the phonons wavelength (Λ). As the sample complexity increases, there is an overall reduction of the phonons mean free path. Inorganic materials (left side) are taken as model systems for biological structures (right side). From the top to the bottom: in vitreous silica and in collagen hydrogels, the phonons probed by Brillouin light scattering feel the system as homogeneous: in these cases, the mean free path, ℓ, is substantially affected only by dynamical attenuation processes. Xerogels are considered the inorganic counterpart of cellular cytoplasm. In this case phonons suffer the presence of structural and elastic heterogeneities, which reduce their mean free path, ℓ. Finally, silica micro and nanoparticles can be taken as model for confined biological structures or isolated systems, such as viruses. In this condition, propagating acoustic modes are not sustained and only localized

normal vibrational modes are present (D < 3-4 Λ). Credit for the virus picture goes to https://www.scientificanimations.com/wiki-images/

In back scattering configuration with a green laser, the broadening of the Brillouin peak measured in bulk v-SiO_2 indicates that the propagation length of the probed phonons, ℓ, is on the order of 40 μm[53]. Therefore, any property measured from the longitudinal Brillouin peak must be considered as representative of the material on this length scale. *It is noteworthy that, considering diffraction limit for visible light, we can reduce the characteristic length of the scattering volume well below 1 μm, but we will in any case observe features averaged on a much larger length scale*.

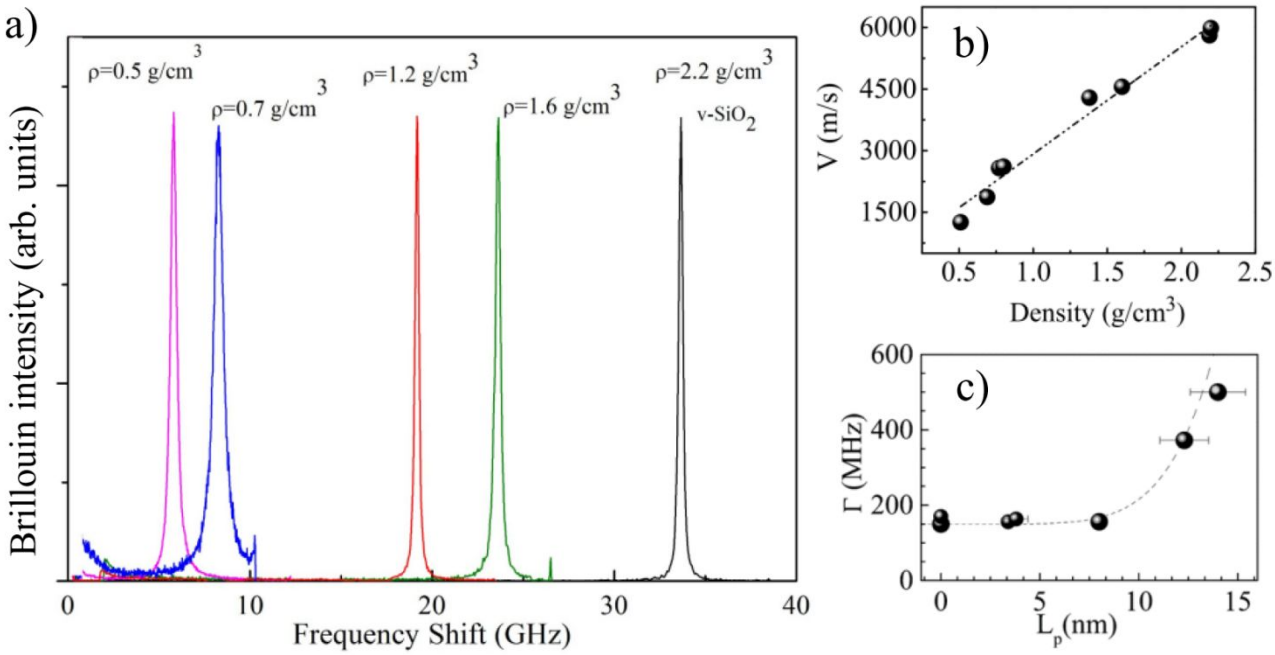

Figure 3: a) Brillouin spectra of silica based samples, with corresponding densities reported inside the figure; b) Longitudinal sound velocity is linearly dependent on the density[54]; c) After a threshold value found at pore size L_p ~ 10 nm, the width of the Brillouin peak increases following a power law dependence[55].

In presence of mechanical interfaces, the macroscopic propagation of acoustic waves modifies according to laws analogous to the refraction and reflection law of the electromagnetic waves, where the acoustic impedance (ρv) takes the role of the dielectric constant, with a clear effect on the propagation length of phonons. In fact, even when the mechanical discontinuities do not form a definite interface because their size is below the phonon wavelength, fluctuations in the mechanical properties induce a *phonon loss of coherence and therefore a lifetime decrease.* This is a frequent case in biological materials where rigid structures, which build up the scaffold, are often intercalated by softer regions, which guarantee easy molecular mobility and nutrient diffusion. A remarkable inorganic model system is offered by xerogels and aerogels: biphasic materials formed by a silica network filled with air[56]. Their synthesis, based on sol-gel process, allows the fine modulation of the structural

features, so that the size and the number of pores can be independently modified. The microscopic structure of the materials has a strong effect on the mechanical properties, and hence on the Brillouin spectra. Representative data are reported in Figure 3 a)[54,55]. The volume fraction of the solid part in these materials influences the position of the peak in the Brillouin spectrum[54], while the peak width is associated to the characteristic size of the voids[54,55]. As a matter of fact, as the pores' size is much smaller than the phonons wavelength, Brillouin spectroscopy feels the system as a single material. The derived sound velocity - linearly dependent on density (Figure 3 b) - is a sort of mean value on the volume, while the width of the Brillouin peak is affected by the degree of elastic disorder of the material which, for the same value of density, increases with the defects size (Figure 3 c). Note that this increase is completely independent from the viscosity of the SiO_2 component. In these systems, increasing the air/SiO_2 discontinuities size above $\lambda/10$ induces a strong elastic light scattering, due to refractive index mismatch, up to a complete loss of q definition, which prevents the study of mechanical properties by BLS. However, in engineered systems where the mechanical modulations are on a larger length scale, such as multilayers or infiltrated opals (i.e. 1D or 3D phononic crystals), but with a reduced index mismatch, it appears that as long as the phonons travel in the two media, the Brillouin measured mechanical properties are averaged[57,58].

In search for a definition of resolution in Brillouin spectroscopy, an operational approach similar to the Rayleigh criterion has to be identified. The question is no longer simply "how far" two single point emitters should be, to be perceived as separate, but "how small" could they be in order to obtain reliable values of the sound velocity in the two separate media?

Multilayers or infiltrated opals present peculiar characteristics in their mechanical properties associated to their structural periodicity, and they are not proper benchmarks to provide the answer. However, as the sample size is reduced, a threshold can be identified below which spontaneous propagating modes are no longer observable. An example can be found studying supported polymeric thin films[59] The threshold, which depends on the phonon wavelength, has been estimated analyzing loose aggregates of silica particles of increasing size: only from 800 nm (corresponding to 3-4 phonon wavelengths) a bulk mode of the single particles was clearly measurable[60]. *It appears that, even if the limit to induce light scattering process by density fluctuations is of the order of the (half) phonon wavelength, this scale is not enough to sustain spontaneous propagating acoustic modes.*

On the other hand, looking at the Brillouin spectrum of microparticles, *localized* acoustic normal modes associated to the particle vibrations are evident when the size of the particles is of the order of the inverse of the exchanged wavevector ($q*D\sim1$)[60–63]. As the frequency of the modes depends on the longitudinal and transverse speed of sound, and it is inversely proportional to the size, the detection of these modes allows a direct evaluation of the *elastic properties of the medium on a length scale in principle much smaller than the scattering volume.* Note that while no propagating mode is observable in the single particle below few Λ, in an assembly of small particles the acoustic modes involving several particles may propagate, and can be measured by Brillouin Scattering or ultrasound techniques. In this case, the speed of sound is related to the interaction mechanism between the particles and can be modulated by changing the contact surface, pressure, an chemical bonds[64–66]. For smaller particles (with size $D << 1/|q|$) normal modes do not give rise to Brillouin scattering (i.e. oscillating modulation of the refractive index on the scale of the wavelength). Instead, during the oscillations, a polarizability modulation arises[67], a mechanism which has a strong similarity with the usual Raman Scattering. It is noteworthy that when scaled down to the nanometer range, the elastic moduli measured by these techniques on solid/unrelaxed samples well compare with measurements by standard techniques on macroscopic samples.

New frontiers for Brillouin imaging: the analysis of biological materials

Micro-Brillouin allows to obtain images with mechanical contrast at the microscale. As an example, Figure 4 (adapted from ref. [68]) shows the elasticity map obtained on living cells (panel a), and a full stack acquired by changing the focal plane along the optical axis while imaging a single cell (panel b). The stiffer region and the nucleoli that fall within the focal plane are visible as red structures and dots, while the background corresponding to medium is reported in black. However, not all the structures of complex biological samples can be actually visualized. The contrast in Brillouin imaging depends both on i) the characteristic dimension of the biological structures, D and ii) the mechanical mismatch between the given structure and the surrounding ones. Furthermore, the spatial resolution of the image depends on the optical focusing due to experimental settings, but it is also influenced by the phonons mean free path, which in turn is related to the properties of the sample and to the phonons wavelength Λ.

In the following, we report on some interesting experiments of biological relevance in which the interplay between the different lengths scales at play is highlighted while decreasing D.

Let's consider the case where the scattering volume V is wholly confined into a single material, and D> ℓ (>3-4 Λ), , being ℓ, the mean free path and Λ the phonons wavelength. This case is sketched in Figure 2a. With respect to inorganic materials, biological matter presents a hierarchical organization, needed for optimizing its functionality preserving all the processes necessary for life. This complexity induces a modulation of mechanical properties on several length scales. In Brillouin scattering, nevertheless, we can consider the medium elastically homogeneous as long as the contribution to the attenuation of the intrinsic viscous effects of the materials dominates that related with the mechanical disorder. This case can be visualized quite well in hydrogel systems: they are networks of hydrophilic polymer chains, whose viscoelastic properties can be finely tuned to mimic those of biological tissues [69]. In the Brillouin analysis, they appear as homogenous systems because the scale of their microstructure is well below the phonon wavelength. However, respect to vitreous silica, the phonons mean free path, ℓ, measured in hydrogels is strongly reduced. In fact, ℓ is affected by the presence of viscous processes, and it assumes values comparable with the ones measured in soft materials or in water, which at room temperature, present ℓ~ 2.5 μm. The effects of viscous processes, mainly related to internal relaxation processes, without introducing any additional elastic heterogeneity in the samples, induces important variations in the phonons mean free path. As recently measured, the dehydration process in collagen hydrogel modifies ℓ, which reaches values comprised between 0.7 and 2.0 μm[70].

Differently from these model systems, in the aforementioned sense, it is questionable whether a real biological material is elastically homogeneous at all. For example, the healthy cornea, which is mostly composed of collagen fibers, could be basically considered as a homogeneous material. Indeed, Brillouin imaging has been successfully applied to diagnose the onset of corneal pathological conditions, by showing changes of the viscoelastic properties, independently by the corneal microstructure. These studies led to the design and implementation of dedicated medical devices based on Brillouin imaging [6 7 64]. However, as recently highlighted even cornea is less elastically homogenous than previously thought. From a recent high resolution Brillouin characterization, the phonon mean free path results of the order of ℓ~1μm [12] and this value provides a lower limit for the actual spatial resolution of mechanical imaging. This ℓ value allows to distinguish the mechanical modulation induced by the presence of collagen sutural lamellae[12] as well as to observe the elastic gradient from the outer edge (the limbus) to the central part[15], or in depth from corneal epithelium to the endothelium[71,72].

It is worth to notice that, many biological materials are far more mechanically disordered than cornea, therefore the actual spatial resolution has to be carefully considered in their Brillouin maps. For example, the elastic

modulus of subcellular components, such as cell nucleus[3,73], nucleoli [74] or intracellular stress granules[6] can be successfully measured only when their characteristic size is greater than the phonons propagation length. Otherwise, the obtained values must be considered an average value of the mechanical properties of the studied structure and the surrounding ones.

Let's consider the case in which the scattering volume comprises two materials of different elastic constants, whose characteristic size is enough to sustain spontaneous propagating acoustic modes (**D > ℓ >3-4 Λ).** In this condition, the sample signal presents two different peaks that co-exist and can be discriminated in the acquired spectrum. This case occurs when mapping the interface between two materials or more in general in the presence of intercalated materials with different enough mechanical properties. Several examples are reported in literature. For example, two spectral features in Brillouin spectra emerged in the analysis of human bone[75] as reported in Figure 5, where the soft and the hard components can be detected disclosing the biphasic nature of the tissue. On a similar note, two components have been observed in the spectra of micro-structured samples composed of wool fibers embedded into an epoxy film[76], of biphasic, amorphous and crystalline ,polymeric film[77], of living cells immersed in their buffer solution[10], in the analysis of a living organisms (zebrafish)[13] and in teeth[14].

In this condition, it is expected that the mechanical transition in the Brillouin image is sharper the higher the acoustic mismatch is[47]. In fact, the lateral resolution in Brillouin imaging is not simply guided by the reduction of the scattering volume, as it occurs in optical microscopy, but an important role is played by the confinement of phonons in that direction. A striking evidence of this complex interplay is provided by the use of high NA objectives that - from one hand - reduces the dimension of the scattering volume, but - on the other hand - is associated to a larger acceptance angle of the objective, that results in a broader range of q probed in the scattering process. The direct effect is a decrease in the selection of the phonons propagation direction, which can also lead to the counterintuitive result of a loss in spatial resolution[47]. Therefore, Brillouin images and the corresponding optical ones (fluorescence, bright field, and also Raman which probes non propagating phonons) *a priori* do not possess the same spatial resolution, even if acquired with the same optics. This effect has been highlighted comparing the Brillouin results with the ones obtained by Raman[47] or fluorescence[7] in a correlative microscopy approach.

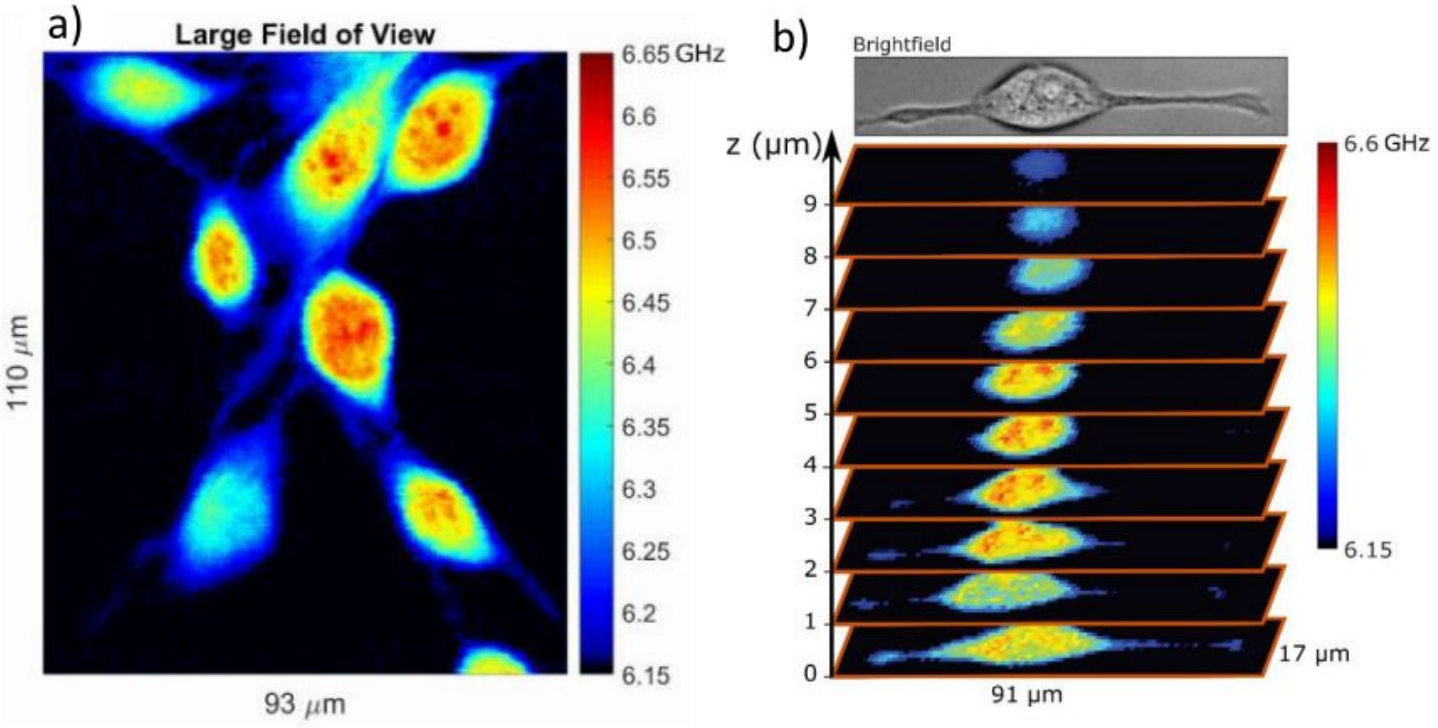

Figure 4: a) Brillouin image of NIH/3T3 cell (murine fibroblasts) deposited on glass the pseudo-colors of the image represent the position of the Brillouin peak. Figure adapted with permission from ref.[68] © The Optical Society. b) 3D Brillouin image of a single NIH/3T3 cell. A series of Brillouin z-scan images of a single cell, attempting to measure the mechanical properties of the cell's internal structure. A bright field microscope image is provided for comparison. Figure adapted with permission from ref.[68] © The Optical Society.

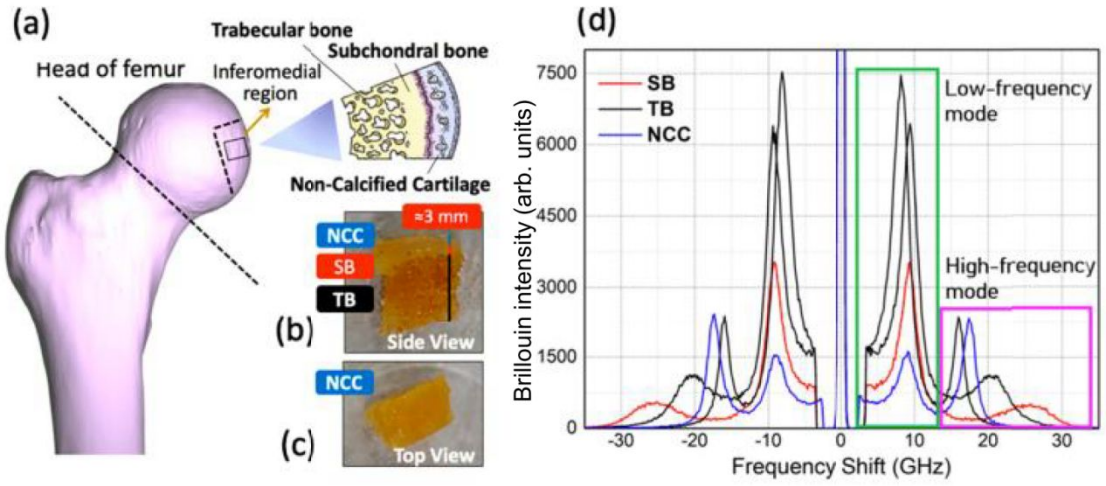

Figure 5: a) Sketch of human femoral head bone. The investigated sample is taken by the so-called interferomedial region, highlighted in figure. Images of the investigated sample are reported in b) and c). The

longitudinal section shows the subchondral (SB), trabecular (TB) and in the highest portion the non-calcified cartilage surface (NCC) part (b), while the top view of the same section, shows the articular non-calcified cartilage surface (NCC) (c). (d) Selected spectra taken in the different zones. Each spectrum shows two peaks associated to the soft and hard components of the bone. Figure adapted with permission from ref.[75]© The Optical Society.

Decreasing the size of D, two limits can be considered. In the first situation (D ~ l and D> 3-4 Λ) the biological structure is composed by a material in which the propagation length should be longer than its actual size. Hence, the phonon propagation will suffer an extra-damping induced by the confinement effect. In the spectrum, while the frequency of the Brillouin peak provides the correct measure of M' of the material, the width of the Brillouin peak provides a mean free path which is smaller than the one expected for the same bulk material, as the shape of the Brillouin peak takes also into account the confinement effect. After a further reduction of D, when the limit D< 3-4 Λ is reached (Figure 2 c)) , propagating acoustics modes are not detectable and only localized normal modes can be measured. The observation of such modes in biological materials is usually prevented by a limited acoustic mismatch. For instance, Sirotkin et al. modeled viruses as homogeneous elastic nanoparticles, but they could not detect the acoustic modes for viruses immersed in their buffer solution[78]. However, such weak scattering modes can be observed by extraordinary acoustic Raman spectroscopy[79] confirming that viruses, from mechanical point of view, can be assimilated to colloidal nanoparticles, whose characteristic modes fall in the GHz range. Based on this observation, the selective resonant excitation of such modes has been recently proposed as an effective virus inactivation method[80], potentially leading to a simple, cost-effective approach to manage broad pandemics as the one we are currently experiencing[81].

The case of **D <Λ** is typically achieved for nano-structures present in the single cell (Figure 2 b)). The cell's cytoplasm for example can be described as a poro-elastic material where a solid-like porous elastic meshwork - the cytoskeleton - is immersed in an interstitial fluid – the cytosol[70]. However, the size of the main cytoskeletal components fall in the nanometer scale, ranging from a diameter of 8-10 nm for actin and intermediate filaments to approximately 30nm for microtubules[82]. This scale is definitely much smaller than the phonons wavelength, and the modifications in the cytoskeleton rigidity cannot be directly tracked by this technique. Nevertheless, their presence affects the phonons propagation and attenuation: if the cells are treated by adding drugs affecting the polymerization level of the cytoskeleton, BLS can observe an overall decrease in the cytoplasmic stiffness[74]. In this case, as in the case of aerogels previously reported, the measure refers to the elastic constant of a single material, which comprises both the cytoskeleton and the cytosol.

Outlook

Brillouin spectroscopy emerged in the recent years as a powerful photonic technique, suitable to obtain images with mechanical contrast at the microscale. Nevertheless, the assessment of BLS as a high resolution optical elastography technique is still in its infancy. The comparison with other more familiar microscopy techniques, and the understanding of similarities and differences, is crucial to unleash the power of the approach, but it requires a careful consideration of the peculiarity of the Brillouin scattering process. In particular, here we addressed the central problem of the spatial resolution achievable in Brillouin imaging. In fact, together with the scattering volume and the wavelength of the excitation beam, the propagating nature of the acoustic phonons imposes to consider their mean free path and their propagation direction. To suitably visualize the results of Brillouin spectroscopy on biological (heterogeneous) samples, it is required to consider the spatial extension of the probed elastic waves as a constitutive element of the analysis, and understand that the resolution is not only

an intrinsic property of the imaging system, but it also depends on the structural and dynamical properties of the sample.

It could be argued that in many cases it is not useful to increase the optical resolution of the Brillouin microscope because of the intrinsic limit on the spatial resolution given by the phonon propagation length. Instead, the full complexity of the light – matter interaction has to be taken into account to identify a suitable route to increase the spatial resolution of the technique. For example, the selective excitation of phonons generated by high power pulsed lasers[38,83] or by a counter-propagating continuous-wave beam[39] have been recently suggested to increase the Brillouin scattering cross-section. These experimental settings, as well as the use of ultrasonic wave patterns within the target material itself[84], are promising but not yet able to overcome the spatial resolution reachable by usual set-ups in spontaneous Brillouin spectroscopy. Promising solutions have been proposed, to tackle the focusing limit of the excitation (the optical one) by laser-assisted thermal lenses[85], or the acoustic resolution by using sub-micron resonators[86]. It is challenging however to apply such solutions to the characterization of biological materials in their functional conditions, because of the intrinsic invasiveness of the techniques.

Very recently, it has been pointed out that the resolution in optical microscopy can be boosted by finely shaping the excitation beam[87]. The same general concept is envisaged to be transferred to tune *the probe-system interaction* in Brillouin imaging. The steering of the optical beam propagation for example can be the experimental key to study mechanically anisotropic materials[88] obtaining a new contrast method in biomechanical imaging. The different elastic properties probed along different directions allow the characterization of the elastic anisotropy in homogeneous as well as heterogeneous materials. As recently demonstrated in tissues[89], the separate investigation of phonons travelling in different directions in an angle-resolved Brillouin experiment can disclose the inherent organization of biological structures opening new frontiers in bio-imaging.

We believe that in the near future Brillouin imaging will have a strong impact in challenging applications of fundamental research in mechanobiology and in clinical diagnostics. However, only the deep understanding of the physical mechanisms driving the material characterization of complex heterogeneous materials will allow to exploit all the potentiality of the technique. The fine experimental control of the interaction mechanisms will direct forthcoming technical developments to optimize new experimental settings for specific bio-photonic applications.

Acknowledgments

We acknowledge the Bio-Brillouin COST Action [CA16124] for the contribution to build a community and a scientific context, which inspired this work. SC acknowledges the Short Term Mobility Program of National Research Council- CNR STM/2019.

Conflict of Interest:

The authors declare that they have no conflict of interest.

Bibliography

(1) Brillouin, L. Diffusion de La Lumière et Des Rayonnes X Par Un Corps Transparent Homogéne; Influence Del´agitation Thermique. Ann. Phys. 1922, 9 (17), 88–122.

(2) L.I. Mandelstam. Light Scattering by Inhomogeneous Media. Zh, Russ. Fiz-Khim. Ova. 1926, 58, 381.

(3) Scarcelli, G.; Polacheck, W. J.; Nia, H. T.; Patel, K.; Grodzinsky, A. J.; Kamm, R. D.; Yun, S. H. Noncontact Three-Dimensional Mapping of Intracellular Hydromechanical Properties by Brillouin Microscopy. Nature Methods 2015, 12 (12), 1132–1134.

(4) Meng, Z.; Traverso, A. J.; Ballmann, C. W.; Troyanova-Wood, M.; Yakovlev, V. V. Seeing Cells in a New Light: A Renaissance of Brillouin Spectroscopy. Advances in Optics and Photonics 2016, 8 (2), 300–327.

(5) Pukhlyakova, E.; Aman, A. J.; Elsayad, K.; Technau, U. β-Catenin-Dependent Mechanotransduction Dates Back to the Common Ancestor of Cnidaria and Bilateria. Proceedings of the National Academy of Sciences of the United States of America 2018, 115 (24), 6231-6236.

(6) Antonacci, G.; de Turris, V.; Rosa, A.; Ruocco, G. Background-Deflection Brillouin Microscopy Reveals Altered Biomechanics of Intracellular Stress Granules by ALS Protein FUS. Communications Biology 2018, 1 (1), 139 DOI: 10.1038/s42003-018-0148-x |.

(7) Elsayad, K.; Werner, S.; Gallemí, M.; Kong, J.; Sánchez Guajardo, E. R.; Zhang, L.; Jaillais, Y.; Greb, T.; Belkhadir, Y. Mapping the Subcellular Mechanical Properties of Live Cells in Tissues with Fluorescence Emission-Brillouin Imaging. Science signaling 2016, 9 (435), rs5 DOI: 10.1126/scisignal.aaf6326.

(8) Shao, P.; Eltony, A. M.; Seiler, T. G.; Tavakol, B.; Pineda, R.; Koller, T.; Seiler, T.; Yun, S. Spatially-Resolved Brillouin Spectroscopy Reveals Biomechanical Abnormalities in Mild to Advanced Keratoconus in Vivo. Scientific Reports 2019, 9 (1), 7467 DOI:10.1038/s41598-019-43811-5.

(9) Scarcelli, G.; Besner, S.; Pineda, R.; Kalout, P.; Yun, S. H. In Vivo Biomechanical Mapping of Normal and Keratoconus Corneas. JAMA Ophthalmology 2015, 133 (4), 480-482.

(10) Mattana, S.; Mattarelli, M.; Urbanelli, L.; Sagini, K.; Emiliani, C.; Serra, M. D.; Fioretto, D.; Caponi, S. Non-Contact Mechanical and Chemical Analysis of Single Living Cells by Microspectroscopic Techniques. Light: Science & Applications 2018, 7 (2), 17139, DOI:10.1038/lsa.2017.139.

(11) Virgone-Carlotta, A.; Dehoux, T.; Mertani, H. C.; Rieu, J.-P.; Rivière, C.; Monnier, S.; Delanoë-Ayari, H.; Dagany, X.; Berthelot, A.; Martinet, Q.; Margueritat, J. High-Frequency Mechanical Properties of Tumors Measured by Brillouin Light Scattering. Physical Review Letters 2019, 122 (1), 018101, DOI: 10.1103/PhysRevLett.122.018101 .

(12) Mercatelli, R.; Mattana, S.; Capozzoli, L.; Ratto, F.; Rossi, F.; Pini, R.; Fioretto, D.; Pavone, F. S.; Caponi, S.; Cicchi, R. Morpho-Mechanics of Human Collagen Superstructures Revealed by All-Optical Correlative Micro-Spectroscopies. Communications Biology 2019, 2 (1), 117 DOI: 10.1038/s42003-019-0357-y .

(13) Bevilacqua, C.; Sánchez-Iranzo, H.; Richter, D.; Diz-Muñoz, A.; Prevedel, R. Imaging Mechanical Properties of Sub-Micron ECM in Live Zebrafish Using Brillouin Microscopy. Biomedical Optics Express 2019, 10 (3), 1420 DOI:10.1364/boe.10.001420.

(14) Lainovic, T.; Margueritat, J.; Martinet, Q.; Dagany, X.; Blažic, L.; Rabasovic, M. D.; Krmpot, A. J.; Dehoux, T. Micromechanical Imaging of Dentin with Brillouin Microscopy. Acta Biomaterialia 2020, 105, 214–222.

(15) Gouveia, R. M.; Lepert, G.; Gupta, S.; Mohan, R. R.; Paterson, C.; Connon, C. J. Assessment of Corneal Substrate Biomechanics and Its Effect on Epithelial Stem Cell Maintenance and Differentiation. Nature Communications 2019, 10, 1496 DOI: 10.1038/s41467-019-09331-6.

(16) Antonacci, G.; Pedrigi, R. M.; Kondiboyina, A.; Mehta, V. V; de Silva, R.; Paterson, C.; Krams, R.; Török, P. Quantification of Plaque Stiffness by Brillouin Microscopy in Experimental Thin Cap Fibroatheroma. Journal of The Royal Society Interface 2015, 12 (112), 20150843 DOI:10.1098/rsif.2015.0843.

(17) Schlüßler, R.; Möllmert, S.; Abuhattum, S.; Cojoc, G.; Müller, P.; Kim, K.; Möckel, C.; Zimmermann, C.; Czarske, J.; Guck, J. Mechanical Mapping of Spinal Cord Growth and Repair in Living Zebrafish Larvae by Brillouin Imaging. Biophysical Journal 2018, 115 (5) 911-923.

(18) Butler, H. J.; Ashton, L.; Bird, B.; Cinque, G.; Curtis, K.; Dorney, J.; Esmonde-White, K.; Fullwood, N. J.; Gardner, B.; Martin-Hirsch, P. L.; Walsh, M. J.; McAinsh, M. R.; Stone, N.; Martin, F. L. Using Raman Spectroscopy to Characterize Biological Materials. Nature Protocols 2016, 11 (4), 664–687.

(19) Prevedel, R.; Diz-Muñoz, A.; Ruocco, G.; Antonacci, G. Brillouin Microscopy - a Revolutionary Tool for Mechanobiology? Nature methods 2019, 16, 969–977.

(20) Mattana, S.; Caponi, S.; Tamagnini, F.; Fioretto, D.; Palombo, F. Viscoelasticity of Amyloid Plaques in Transgenic Mouse Brain Studied by Brillouin Microspectroscopy and Correlative Raman Analysis. Journal of Innovative Optical Health Sciences 2017, 10 (6) 1742001 DOI: 10.1142/S1793545817420019.

(21) Koski, K. J.; Akhenblit, P.; McKiernan, K.; Yarger, J. L. Non-Invasive Determination of the Complete Elastic Moduli of Spider Silks. Nature Materials 2013, 12 (3), 262–267.

(22) Schneider, D.; Gomopoulos, N.; Koh, C. Y.; Papadopoulos, P.; Kremer, F.; Thomas, E. L.; Fytas, G. Nonlinear Control of High-Frequency Phonons in Spider Silk. Nature Materials 2016, 15 (10) 1079-1083.

(23) Wang, Z.; Cang, Y.; Kremer, F.; Thomas, E. L.; Fytas, G. Determination of the Complete Elasticity of Nephila Pilipes Spider Silk. Biomacromolecules 2020, 21 (3), 1179–1185.

(24) Caponi, S.; Corezzi, S.; Mattarelli, M.; Fioretto, D. Stress Effects on the Elastic Properties of Amorphous Polymeric Materials. Journal of Chemical Physics 2014, 141 (21) 214901 DOI: 10.1063/1.4902060.

(25) Bottani, C. E.; Fioretto, D. Advances in Physics : X Brillouin Scattering of Phonons in Complex Materials. Advances in Physics: X 2018, 3 (1) 1467281 DOI: 10.1080/23746149.2018.1467281.

(26) Comez, L.; Masciovecchio, C.; Monaco, G.; Fioretto, D. Progress in Liquid and Glass Physics by Brillouin Scattering Spectroscopy. In Solid State Physics - Advances in Research and Applications; 2012; Vol. 63, pp 1–77.

(27) Vacher, R.; Pelous, J.; Courtens, E. Mean Free Path of High-Frequency Acoustic Excitations in Glasses with Application to Vitreous Silica. Physical Review B - Condensed Matter and Materials Physics 1997, 56 (2), R481–R484.

(28) LePesant, J.-P.; Powers, L.; Pershan, P. S. Brillouin Light Scattering Measurement of the Elastic Properties of Aligned Multilamella Lipid Samples. Proceedings of the National Academy of Sciences 1978, 75 (4), 1792–1795.

(29) Cusack, S.; Miller, A. Determination of the Elastic Constants of Collagen by Brillouin Light Scattering. Journal of Molecular Biology 1979, 135 (1), 39–51.

(30) Koski, K. J.; Yarger, J. L. Brillouin Imaging. Applied Physics Letters 2005, 87 (6), 061903 DOI: 10.1063/1.1999857.

(31) Coker, Z.; Troyanova-Wood, M.; Traverso, A. J.; Yakupov, T.; Utegulov, Z. N.; Yakovlev, V. V. Assessing Performance of Modern Brillouin Spectrometers. Optics Express 2018, 26 (3), 2400, doi: 10.1364/OE.26.002400.

(32) Meng, Z.; Bustamante Lopez, S. C.; Meissner, K. E.; Yakovlev, V. V. Subcellular Measurements of Mechanical and Chemical Properties Using Dual Raman-Brillouin Microspectroscopy. Journal of Biophotonics 2016, 9 (3), 201–207.

(33) Meng, Z.; Yakovlev, V. V. Precise Determination of Brillouin Scattering Spectrum Using a Virtually Imaged Phase Array (VIPA) Spectrometer and Charge-Coupled Device (CCD) Camera. 2016, 70 (8), 1356–1363.

(34) Fiore, A.; Zhang, J.; Shao, P.; Yun, S. H.; Scarcelli, G. High-Extinction Virtually Imaged Phased Array-Based Brillouin Spectroscopy of Turbid Biological Media. Applied Physics Letters 2016, 108 (20), 203701, DOI: 10.1063/1.4948353

(35) Scarcelli, G.; Yun, S. H. Multistage VIPA Etalons for High-Extinction Parallel Brillouin Spectroscopy. Optics Express 2011 (11) 10913 DOI: 10.1364/oe.19.010913.

(36) Scully, M. O.; Thompson, J. V.; Yakovlev, V. V.; Traverso, A. J.; Ballmann, C. W.; Meng, Z. Stimulated Brillouin Scattering Microscopic Imaging. Scientific Reports 2015, 5 (1), 18139 DOI: 10.1038/srep18139.

(37) Remer, I.; Bilenca, A. High-Speed Stimulated Brillouin Scattering Spectroscopy at 780 Nm. APL Photonics 2016, 1 (6) 061301 DOI: 10.1063/1.4953620.

(38) Ballmann, C. W.; Meng, Z.; Traverso, A. J.; Scully, M. O.; Yakovlev, V. V. Impulsive Brillouin Microscopy. Optica 2017, 4 (1), 124-128.

(39) Remer, I.; Bilenca, A. Background-Free Brillouin Spectroscopy in Scattering Media at 780 Nm via Stimulated Brillouin Scattering. Optics Letters 2016, 41 (5), 926-929.

(40) Scarponi, F.; Mattana, S.; Corezzi, S.; Caponi, S.; Comez, L.; Sassi, P.; Morresi, A.; Paolantoni, M.; Urbanelli, L.; Emiliani, C.; Roscini, L.; Corte, L.; Cardinali, G.; Palombo, F.; Sandercock, J. R.; Fioretto, D. High-Performance Versatile Setup for Simultaneous Brillouin-Raman Microspectroscopy. Physical Review X 2017, 7 (3) 031015 DOI: 10.1103/PhysRevX.7.031015.

(41) Zhang, J.; Fiore, A.; Yun, S.; Kim, H.; Scarcelli, G. Line-Scanning Brillouin Microscopy for Rapid Non-Invasive Mechanical Imaging. Nature Publishing Group 2016, 6 (1) 35398 DOI: 10.1038/srep35398.

(42) Klar, T. A.; Jakobs, S.; Dyba, M.; Egner, A.; Hell, S. W. Fluorescence Microscopy with Diffraction Resolution Barrier Broken by Stimulated Emission. Proceedings of the National Academy of Sciences of the United States of America 2000, 97 (15), 8206–8210.

(43) Masullo, L. A.; Bodén, A.; Pennacchietti, F.; Coceano, G.; Ratz, M.; Testa, I. Enhanced Photon Collection Enables Four Dimensional Fluorescence Nanoscopy of Living Systems. Nature Communications 2018, 9 (1) 3281 DOI: 10.1038/s41467-018-05799-w.

(44) Pennacchietti, F.; Serebrovskaya, E. O.; Faro, A. R.; Shemyakina, I. I.; Bozhanova, N. G.; Kotlobay, A. A.; Gurskaya, N. G.; Bodén, A.; Dreier, J.; Chudakov, D. M.; Lukyanov, K. A.; Verkhusha, V. V.; Mishin, A. S.; Testa, I. Fast Reversibly Photoswitching Red Fluorescent Proteins for Live-Cell RESOLFT Nanoscopy. Nature Methods 2018, 9 (1) 3281 DOI:10.1038/s41467-018-05799-w.

(45) Smolyaninov, I. I.; Elliott, J.; Zayats, A. V.; Davis, C. C. Far-Field Optical Microscopy with a Nanometer-Scale Resolution Based on the in-Plane Image Magnification by Surface Plasmon Polaritons. Physical Review Letters 2005, 94 (5), 057401, DOI: 10.1103/PhysRevLett.94.057401.

(46) Novotny, L.; Stranick, S. J. Near-Field Optical Microscopy and Spectroscopy With Pointed Probes. Annual Review of Physical Chemistry 2005, 57 (1), 303–331.

(47) Caponi, S.; Fioretto, D.; Mattarelli, M. On the Actual Spatial Resolution of Brillouin Imaging. Optics Letters 2020, 45 (5), 1063-1066.

(48) Palombo, F.; Fioretto, D. Brillouin Light Scattering: Applications in Biomedical Sciences. Chemical Reviews 2019, 119 (13), 7833–7847.

(49) Scopigno, T.; Ruocco, G.; Sette, F. Microscopic Dynamics in Liquid Metals: The Experimental Point of View. Reviews of Modern Physics 2005, 77 (3), 881–933.

(50) Ruocco, G.; Sette, F.; Di Leonardo, R.; Fioretto, D.; Krisch, M.; Lorenzen, M.; Masciovecchio, C.; Monaco, G.; Pignon, F.; Scopigno, T. Nondynamic Origin of the High-Frequency Acoustic Attenuation in Glasses. Physical Review Letters 1999, 83 (26), 5583–5586.

(51) Marruzzo, A.; Schirmacher, W.; Fratalocchi, A.; Ruocco, G. Heterogeneous Shear Elasticity of Glasses: The Origin of the Boson Peak. Scientific Reports 2013, 3, 1407 DOI: 10.1038/srep01407.

(52) Schirmacher, W.; Ruocco, G.; Scopigno, T. Acoustic Attenuation in Glasses and Its Relation with the Boson Peak. Physical Review Letters 2007, 98 (2), 025501 DOI: 10.1103/PhysRevLett.98.025501.

(53) Vacher, R.; Pelous, J. Behavior of Thermal Phonons in Amorphous Media from 4 to 300 K. Physical Review B 1976, 14 (2), 823–828.

(54) Caponi, S.; Carini, G.; D'Angelo, G.; Fontana, A.; Pilla, O.; Rossi, F.; Terki, F.; Tripodo, G.; Woignier, T. Acoustic and Thermal Properties of Silica Aerogels and Xerogels. Physical Review B 2004, 70 (21), 214204 DOI: 10.1103/PhysRevB.70.214204.

(55) Caponi, S.; Benassi, P.; Eramo, R.; Giugni, A.; Nardone, M.; Fontana, A.; Sampoli, M.; Terki, F.; Woignier, T. Phonon Attenuation in Vitreous Silica and Silica Porous Systems. Philosophical Magazine 2004, 84 (13-16) 1423–1431.

(56) Gurav, J. L.; Jung, I.-K.; Park, H.-H.; Kang, E. S.; Nadargi, D. Y. Silica Aerogel: Synthesis and Applications. Journal of Nanomaterials 2010, 2010, 409310 , 1–11.

(57) Cheng, W.; Wang, J.; Jonas, U.; Fytas, G.; Stefanou, N. Observation and Tuning of Hypersonic Bandgaps in Colloidal Crystals. Nature Materials 2006, 5 (10), 830–836.

(58) Hotz, R.; Krüger, J. K.; Siems, R. Brillouin Scattering in Layered Structures. Solid State Communications 1983, 46 (2), 155–158.

(59) Gomopoulos, N.; Cheng, W.; Efremov, M.; Nealey, P. F.; Fytas, G. Out-of-Plane Longitudinal Elastic Modulus of Supported Polymer Thin Films. Macromolecules 2009, 42 (18) 7164-7167.

(60) Lim, H. S.; Kuok, M. H.; Ng, S. C.; Wang, Z. K. Brillouin Observation of Bulk and Confined Acoustic Waves in Silica Microspheres. Applied Physics Letters 2004, 84 (21), 4182–4184.

(61) Still, T.; Mattarelli, M.; Kiefer, D.; Fytas, G.; Montagna, M. Eigenvibrations of Submicrometer Colloidal Spheres. Journal of Physical Chemistry Letters 2010, 1 (16), 2440–2444.

(62) Montagna, M. Brillouin and Raman Scattering from the Acoustic Vibrations of Spherical Particles with a Size Comparable to the Wavelength of the Light. Physical Review B - Condensed Matter and Materials Physics 2008, 77 (4), 045418, DOI: 10.1103/PhysRevB.77.045418.

(63) Mattarelli, M.; Montagna, M. Comment on “Selection Rules for Brillouin Light Scattering from Eigenvibrations of a Sphere” [Chem. Phys. Lett. 461 (2008) 111]. Chemical Physics Letters 2012, 524, 112–115.

(64) Mattarelli, M.; Montagna, M.; Still, T.; Schneider, D.; Fytas, G. Vibration Spectroscopy of Weakly Interacting Mesoscopic Colloids. Soft Matter 2012, 8 (15), 4235–4243.

(65) Girard, A.; Gehan, H.; Crut, A.; Mermet, A.; Saviot, L.; Margueritat, J. Mechanical Coupling in Gold Nanoparticles Supermolecules Revealed by Plasmon-Enhanced Ultralow Frequency Raman Spectroscopy. Nano Letters 2016, 16 (6), 3843–3849.

(66) Ayouch, A.; Dieudonné, X.; Vaudel, G.; Piombini, H.; Vallé, K.; Gusev, V.; Belleville, P.; Ruello, P. Elasticity of an Assembly of Disordered Nanoparticles Interacting via Either Van Der Waals-Bonded or Covalent-Bonded Coating Layers. ACS Nano 2012, 6 (12), 10614–10621.

(67) Mattarelli, M.; Montagna, M.; Rossi, F.; Chiasera, A.; Ferrari, M. Mechanism of Low-Frequency Raman Scattering from the Acoustic Vibrations of Dielectric Nanoparticles. Physical Review B - Condensed Matter and Materials Physics 2006, 74 (15), 153412 DOI: 10.1103/PhysRevB.74.153412.

(68) Nikolić, M.; Scarcelli, G. Long-Term Brillouin Imaging of Live Cells with Reduced Absorption-Mediated Damage at 660nm Wavelength. Biomedical Optics Express 2019, 10 (4), 1567-1580.

(69) Re, F.; Sartore, L.; Moulisova, V.; Cantini, M.; Almici, C.; Bianchetti, A.; Chinello, C.; Dey, K.; Agnelli, S.; Manferdini, C.; Bernardi, S.; Lopomo, N. F.; Sardini, E.; Paganelli, C.; Guizzi, P.; Lisignoli, G. Combined with Human Platelet Lysate Highly Support Human Mesenchymal Stem Cell Proliferation and Osteogenic Differentiation. 2019, 10, 204173141984585 DOI: 10.1177/2041731419845852.

(70) Bailey, M.; Alunni-Cardinali, M.; Correa, N.; Caponi, S.; Holsgrove, T.; Barr, H.; Stone, N.; Winlove, C. P.; Fioretto, D.; Palombo, F. Brillouin-Derived Viscoelastic Parameters of Hydrogel Tissue Models. arXiv 2020 , arXiv:1912.08292.

(71) Lepert, G.; Gouveia, R. M.; Connon, C. J.; Paterson, C. Assessing Corneal Biomechanics with Brillouin Spectro-Microscopy. Faraday Discussions 2016, 187, 415–428.

(72) Scarcelli, G.; Kling, S.; Quijano, E.; Pineda, R.; Marcos, S.; Yun, S. H. Brillouin Microscopy of Collagen Crosslinking: Noncontact Depth-Dependent Analysis of Corneal Elastic Modulus. Investigative Ophthalmology and Visual Science 2013, 54 (2) 1418-1425.

(73) Zhang, J.; Alisafaei, F.; Nikolić, M.; Nou, X. A.; Kim, H.; Shenoy, V. B.; Scarcelli, G. Nuclear Mechanics within Intact Cells Is Regulated by Cytoskeletal Network and Internal Nanostructures. Small 2020, 16 (18), 1907688 DOI: 10.1002/smll.201907688.

(74) Antonacci, G.; Braakman, S. Biomechanics of Subcellular Structures by Non-Invasive Brillouin Microscopy. Scientific Reports 2016, 6, 37217 DOI: 10.1038/srep37217.

(75) Cardinali, M. A.; Dallari, D.; Govoni, M.; Stagni, C.; Marmi, F.; Tschon, M.; Brogini, S.; Fioretto, D.; Morresi, A. Brillouin Micro-Spectroscopy of Subchondral, Trabecular Bone and Articular Cartilage of the Human Femoral Head. Biomedical Optics Express 2019, 10 (5), 2606-2611.

(76) Fioretto, D.; Caponi, S.; Palombo, F. Brillouin-Raman Mapping of Natural Fibers with Spectral Moment Analysis. Biomedical Optics Express 2019, 10 (3), 1469-1474.

(77) Priadilova, O.; Cheng, W.; Tommaseo, G.; Steffen, W.; Gutmann, J. S.; Fytas, G. Probing the Micromechanical Behavior of Semicrystalline Polypropylene Films by Brillouin Spectroscopy. Macromolecules 2005, 38 (6) 2321-2326.

(78) Sirotkin, S.; Mermet, A.; Bergoin, M.; Ward, V.; Van Etten, J. L. Viruses as Nanoparticles: Structure versus Collective Dynamics. Physical Review E - Statistical, Nonlinear, and Soft Matter Physics 2014, 90 (2), 022718, DOI: 10.1103/PhysRevE.90.022718.

(79) Burkhartsmeyer, J.; Wang, Y.; Wong, K. S.; Gordon, R. Optical Trapping, Sizing, and Probing Acoustic Modes of a Small Virus. Applied Sciences (Switzerland) 2020, 10 (1) 394 DOI:10.3390/app10010394.

(80) Yang, S. C.; Lin, H. C.; Liu, T. M.; Lu, J. T.; Hung, W. T.; Huang, Y. R.; Tsai, Y. C.; Kao, C. L.; Chen, S. Y.; Sun, C. K. Efficient Structure Resonance Energy Transfer from Microwaves to Confined Acoustic Vibrations in Viruses. Scientific Reports 2015, 5 (1), 18030, DOI: 10.1038/srep18030.

(81) Cyranoski, D. Profile of a Killer: The Complex Biology Powering the Coronavirus Pandemic. Nature 2020, 581 (7806), 22–26.

(82) Milo, R., Phillips, R. Cell Biology by the Numbers. The Quarterly Review of Biology New York: Garland Science, 2015 92 (4) DOI:10.1201/9780429258770

(83) Krug, B.; Koukourakis, N.; Czarske, J. W. Impulsive Stimulated Brillouin Microscopy for Non-Contact, Fast Mechanical Investigations of Hydrogels. Optics Express 2019, 27 (19), 26910.

(84) Scopelliti, M. G.; Chamanzar, M. Ultrasonically Sculpted Virtual Relay Lens for in Situ Microimaging. Light: Science and Applications 2019, 8 (1) 65 doi: 10.1038/s41377-019-0173-7.

(85) Edrei, E.; Scarcelli, G. Optical Focusing beyond the Diffraction Limit via Vortex-Assisted Transient Microlenses. ACS Photonics 2020, 7 (4) 914-918.

(86) Dehoux, T.; Ishikawa, K.; Otsuka, P. H.; Tomoda, M.; Matsuda, O.; Fujiwara, M.; Takeuchi, S.; Veres, I. A.; Gusev, V. E.; Wright, O. B. Optical Tracking of Picosecond Coherent Phonon Pulse Focusing inside a Sub-Micron Object. Light: Science and Applications 2016, 5 (5), e16082, doi:10.1038/lsa.2016.82.

(87) Breedijk, R. M. P.; Wen, J.; Krishnaswami, V.; Bernas, T.; Manders, E. M. M.; Setlow, P.; Vischer, N. O. E.; Brul, S. A Live-Cell Super-Resolution Technique Demonstrated by Imaging Germinosomes in Wild-Type Bacterial Spores. Scientific Reports 2020 10 (1) 5312 DOI:10.1038/s41598-020-62377-1.

(88) Elsayad, K.; Urstöger, G.; Czibula, C.; Teichert, C.; Gumulec, J.; Balvan, J.; Pohlt, M.; Hirn, U. Mechanical Properties of Cellulose Fibers Measured by Brillouin Spectroscopy. Cellulose 2020, 27 (8) 4209-4220.

(89) Eltony, A. M.; Shao, P.; Yun, S.-H. Measuring Mechanical Anisotropy of the Cornea with Brillouin Microscopy. 2020, arXiv:2003.04344 .

For Table of Contents Use Only

Relevant length scales in Brillouin imaging of biomaterials: the interplay between phonons propagation and light focalization

Maurizio Mattarelli[1], Massimo Vassalli [2], Silvia Caponi [32]*

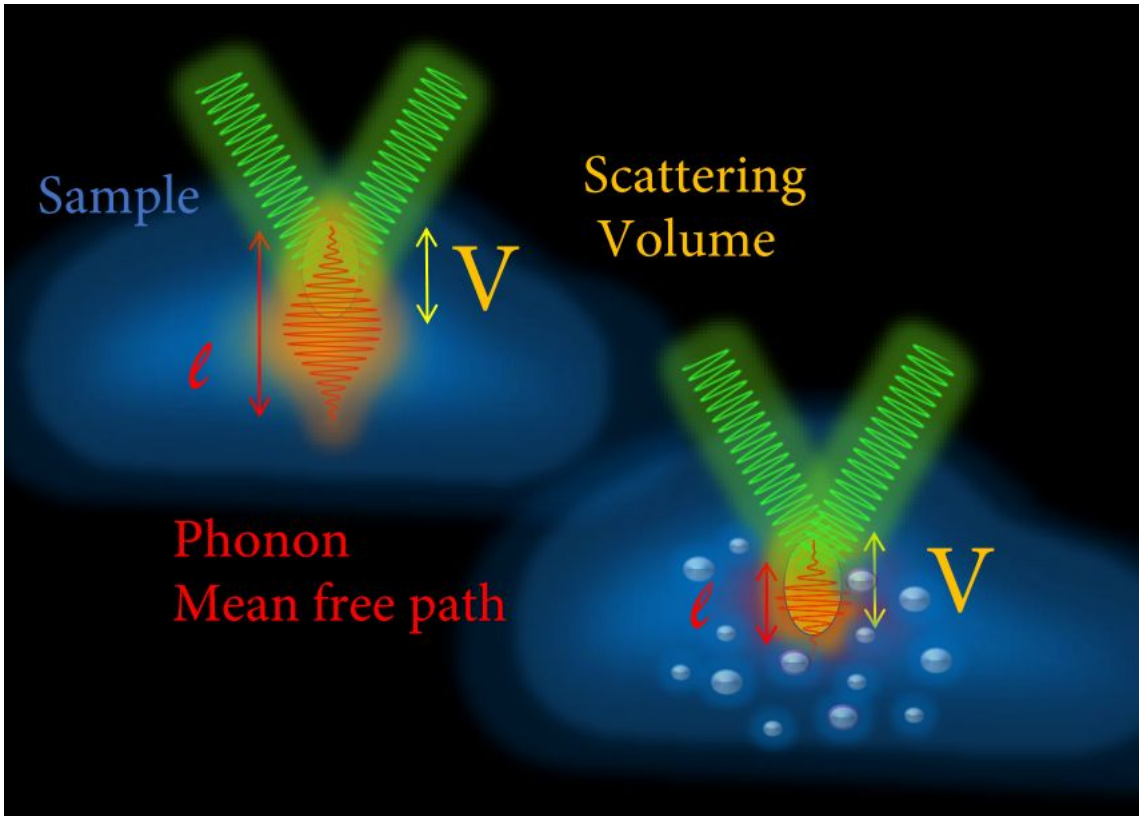

TOC: The figure reports the modification of the phonons mean free path (reported as red damped oscillation) in the case of homogeneous material (upper sketched) and in the case of material where heterogeneity are present (lower sketched). V is the optical scattering volume and it is reported in yellow, while the green waves represent the incoming and outcoming photons.

* corresponding author: silvia.caponi@cnr.it